Original Article

Calculation of Organ Dose Distribution (in-field and Out-of-field) in Breast Cancer Radiotherapy on RANDO Phantom Using GEANT4 Application for Tomographic Emission (Gate) Monte Carlo Simulation

Abstract

Introduction: Organ dose distribution calculation in radiotherapy and knowledge about its side effects in cancer etiology is the most concern for medical physicists. Calculation of organ dose distribution for breast cancer treatment plans with Monte Carlo (MC) simulation is the main goal of this study. **Materials and Methods:** Elekta Precise linear accelerator (LINAC) photon mode was simulated and verified using the GEANT4 application for tomographic emission. Eight different radiotherapy treatment plans on RANDO's phantom left breast were produced with the ISOgray treatment planning system (TPS). The simulated plans verified photon dose distribution in clinical tumor volume (CTV) with TPS dose volume histogram (DVH) and gamma index tools. To verify photon dose distribution in out-of-field organs, the point dose measurement results were compared with the same point doses in the MC simulation. Eventually, the DVHs for out-of-field organs that were extracted from the TPS and MC simulation were compared. **Results:** Based on the implementation of gamma index tools with 2%/2 mm criteria, the simulated LINAC output demonstrated high agreement with the experimental measurements. Plan simulation for in-field and out-of-field organs had an acceptable agreement with TPS and experimental measurement, respectively. There was a difference between DVHs extracted from the TPS and MC simulation for out-of-field organs in low-dose parts. This difference is due to the inability of the TPS to calculate dose distribution in out-of-field organs. **Conclusion and Discussion:** Based on the results, it was concluded that the treatment plans with the MC simulation have a high accuracy for the calculation of out-of-field dose distribution and could play a significant role in evaluating the important role of dose distribution for second primary cancer estimation.

Keywords: *Breast cancer, dosimetry, Monte Carlo simulation, radiation therapy, second primary cancer*

Submitted: 12-Jun-2023 **Revised:** 02-Feb-2024 **Accepted:** 05-Mar-2024 **Published:** 10-Jul-2024

Marziyeh Behmadi[1,2], Mohammad Taghi Bahreyni Toossi[3,4], Shahrokh Nasseri[3,4], Mohammad Ehsan Ravari[1,2], Mahdi Momennezhad[5], Hamid Gholamhosseinian[3,4], Mohammad Mohammadi[6], Sibusiso Mdletshe[7]

[1]Cancer Research Center, Semnan University of Medical Sciences, [2]Department of Medical Physics, Faculty of Medicine, Semnan University of Medical Sciences, Semnan, [3]Department of Medical Physics, Faculty of Medicine, Mashhad University of Medical Sciences, [4]Medical Physics Research Center, Mashhad University of Medical Sciences, [5]Nuclear Medicine Research Center, Mashhad University of Medical Sciences, Mashhad, Iran, [6]Department of Medical Physics, Royal Adelaide Hospital, Adelaide, Australia, [7]Department of Anatomy and Medical Imaging, Faculty of Medical and Health Sciences, University of Auckland, Auckland, New Zealand

Address for correspondence:
Dr. Mohammad Mohammadi, Department of Medical Physics, Royal Adelaide Hospital, Adelaide, SA, Australia. School of Physical Sciences, The University of Adelaide, Adelaide, SA, Australia. E-mail: mohammad.mohammadi@sa.gov.au

Introduction

Radiation-induced second cancer is an important radiation therapy; late effect is a major concern and several studies have been conducted to study this phenomenon.[1-11] One of the important parameters for modeling and estimating the risk of radiation-induced second cancer is dose distribution in organs that are out-of-field of radiation treatment, i.e. outside the target volume. This dose could be due to radiation leakage from the head of the medical linear accelerator (LINAC), scatter from the beam collimators, and scatter within the patient.[12]

The treatment planning system (TPS), experimental dosimetry in a standard phantom, and Monte Carlo (MC) calculations simulation are used to measure organ doses. TPS calculates the in-field (target volume) dose distribution accurately but the calculation does not have enough accuracy for organ dose distribution that is outside the target volume.[12-17] Experimental measurements can be used only on the standard phantoms with passive dosimeters.[12,18-22] Several authors have measured doses of in-field and out-of-field organs in physical phantoms with passive detectors and compared their results with the TPS results.[8,12,21-25] All the investigators reported that the TPS cannot calculate the out-of-field dose accurately and the gold standard method to estimate this dose is MC simulation based on a patient's DICOM data or using computational phantom.[12,17,26-29] Bednarz *et al.*,[26] Joosten

How to cite this article: Behmadi M, Toossi MT, Nasseri S, Ravari ME, Momennezhad M, Gholamhosseinian H, *et al.* Calculation of organ dose distribution (in-field and Out-of-field) in breast cancer radiotherapy on RANDO phantom using GEANT4 application for tomographic emission (Gate) Monte carlo simulation. J Med Signals Sens 2024;14:18.

Access this article online

Website: www.jmssjournal.net

DOI: 10.4103/jmss.jmss_25_23

Quick Response Code:

et al.,[16] Berris *et al.*,[27] and Wang and Ding (2014)[30] evaluated the out-of-field dose calculated by different TPS and used the MC simulation to estimate the uncertainties of calculated organ doses. However, these studies did not compare the in-field dose distribution to verify the primary treatment plan simulations and did not report the dose volume histograms (DVHs) for the organs (in-field and out-of-field) in their studies.

The specific goals of the current study are to calculate and compare the dose distribution for in-field and out-of-field organs for breast cancer patients treated with conformal radiation therapy techniques for eight different treatment planes and two different photon energies. The in-field dose distribution was calculated with the TPS and MC simulation while the out-of-field dose distribution was measured and calculated with thermoluminescent dosimeters (TLDs) and MC simulation, respectively. To calculate the dose distribution, the prescribed dose was delivered to the isocenter point based on the calculated monitor unit (MU) of the TPS for each field. This approach has not been used in previous studies.

Materials and Methods

The study was performed on a RANDO phantom, and therefore, did not need ethical approval.

LINAC modeling and verification of model

The Elekta Precise LINAC (Stockholm, Sweden) photon mode (energy 6 MV and 15 MV) was simulated with GEANT4 application for tomographic emission (GATE) (version 7.2, Gate Collaboration, Lyon, France) MC simulation. Verification of the LINAC was done in two steps: (1) determining the energy spectrum of the electron source and (2) calculating the percentage depth dose (PDD) and dose profile in 10-cm depth for three different fields (6 × 6, 10 × 10, and 20 cm × 20 cm).

Percentage depth dose and dose profile from experimental measurement

Experimental data were measured with a Wellhofer-Scanditronix dosimetry system (Wellhofer, Uppsala, Sweden) and a water phantom with a 50 cm × 50 cm × 50 cm dimension (RFA-300; IBA Dosimetry GmbH, Schuarzenbruck, Germany). PDDs and dose profiles in 10 cm depth were measured for three different field sizes in Wellhofer-Scanditronix's water phantom.

Determining the energy spectrum of the electron source

Finding the energy spectrum for both energies (6 and 15 MV) based on the build-up region in the central axis of the reference field (10 cm × 10 cm) on PDD and dose profile was the first step after modeling the geometry. In regard to the LINAC experimental data, the energy spectrum for both nominal energies was determined using the standard procedure of comparing the measured PDD and the calculated PDD.

Calculating percentage depth dose and dose profile in 10-centimeter depth for three different fields

To perform dose calculations in a water phantom within the simulation code, the same condition of experimental measurement was written in codes. The output of GATE codes was read with MATLAB software (version 2016, MathWorks, California, U.S.) and the data were extracted. To accomplish a good agreement and reduce the uncertainty in water phantom voxels, the codes were run in two steps. Step 1: 3×10^8 particles were run from the electron source to have at least 10^8 particles on the phase space volume. Step 2: for the codes without wedge, 2×10^{10} particles and for the codes with wedge, 4×10^{10} particles were run from the phase space to reduce the uncertainty in the phantom voxels and fluctuation in profiles. The results were compared with experimental measurements using the gamma index with 2%/2 mm criteria.

RANDO phantom in Monte Carlo simulation of treatment plans

Treatment plans on RANDO phantom with the treatment planning system

To estimate and compare the organ's dose distributions (in-field and out-of-field), RANDO Alderson phantom computed tomography images imported to ISOgray TPS (version 4.2.3.50 L, DosiSoft, Paris, France) in the previous study,[31] were used. In the previous study, the authors produced eight different plans [Table 1] on the phantom's left breast in two techniques (conformal techniques in the presence of a dedicated shield [conventional] or multi-leaf collimator [MLC]) and two different photon energies (6 and 15 MV). Planning involved contouring of 15 organs at risk (OAR) (left and right breast, right and left lenses, thyroid, right and left lung, right and left kidney, spinal cord, heart and liver, bladder, rectum, uterus) by the radiation oncologist on DICOM images in the TPS. The treatment plans were produced for 6MV and 15 MV photon beams using conformal radiation therapy techniques in the presence of dedicated shield or MLC, for two opposed tangential fields and two opposed tangential fields plus supraclavicular and postaxial fields.[31] The prescribed dose was 50 Gy in 25 fractions prescribed to the isocenter.

Simulation of treatment plans on RANDO phantom with Monte Carlo

The same plans were simulated with GATE. The phantom's DICOMs were converted to interfile (h33 and i33 files) format with (X) Med-Con software (version 0.14.1, Erick Nolf, Ghent University Hospital, Ghent, Belgium) and MC codes were prepared to read the phantom files. All details of plans were modeled in MC codes. The programs were run in two steps and the voxel size for the phantom was

selected as 3 mm × 3 mm × 3 mm. In regard to the Elekta LINACs universal wedge with 60°, for treatment fields on plans with a lower degree of the wedge on the beam way, two separate programs were written and run (with and without wedge).

Comparison between treatment planning system and GEANT4 application for tomographic emission Monte Carlo simulation for in-field dose verification

The programs for different fields of each plan were run for 5×10^{10} particles and radiation dose distribution in organs was calculated. The dose uncertainty for all fields in eight plans was <0.7% and 2% in in-field and out-of-field, respectively. The results for different fields of each plan obtained from MC simulation were added with MATLAB and then normalized to the prescribed dose voxel. The weight for each field was applied based on the MU.

To have the real dose distribution in plans, for all normalized dose distribution matrixes obtained from simulation, total matrix doses were multiplied to a specific registered number for each treatment plan to have the acceptable dose distribution (95% of the volume received 95% of the prescribed dose) inside the CTV. According to this dose distribution in CTV, dose distribution to the other organs could be estimated. The normalized matrixes of doses calculated with MC code and the TPS were evaluated with a three-dimensional (3D) gamma index MATLAB m-file.[32] The comparison was done inside the treatment fields based on two points as follows: (1) a mask was designed with MATLAB m-file to compare the in-field dose distribution (the area that received at least 40% of the prescribed dose). The defined area is greater than the CTV; (2) due to the difference in the dose calculation algorithm in the TPS and MC simulation, with knowledge of the complexity of the breast cancer treatment fields, the authors selected 3%/3 mm to 6%/6 mm gamma index criteria for dose difference (DD) and distance to agreement (DTA).

To calculate and compare the DVHs for the TPS and MC simulation dose distributions, a 3DSlicer (version 4.10.0, Brigham and Women's Hospital, Boston, MA, USA)[33] was used. In the first step, to calculate the dose distribution with 3DSlicer, the same techniques done with MATLAB were used with a simple filters' module (The Shift Scale Image Filter and Add Image Filter) in the RTSlicer extension of this software. This was followed by the use of the DVH comparison module in 3DSlicer was used to draw the DVHs for both the MC simulation and the TPS. To achieve this, the software needs the radiotherapy computed tomography (RTCT), RT structure, and dose distribution (RT dose). The DD and DTA criteria for CTVs' DVH comparison with the 3DSlicer were selected to be 1% and 1 mm, respectively.

Out-of-field photon dose distribution verification

To verify the photon dose distribution for the out-of-field treatment volumes, measured point doses reported in the previous study[31] were used.

Comparison between point dose measurement and Monte Carlo simulation results

The point doses were measured with TLD chips (MTS 700, TLD Poland, Krakow, Poland) in 48 points and 13 OAR. The RTCT, RT structure, and MC dose distribution 3D matrix files were uploaded and overlaid with the 3DSlicer. According to this overlay, the MC simulation point dose results were compared with the same measurement point dose results and report.

Comparison between treatment planning system and Monte Carlo simulation dose volume histograms for out-of-field organs

Based on the knowledge that the TPSs do not have enough accuracy for dose distribution calculation in out-of-field organs,[12-17] as the last step in this study, the out-of-field organs DVHs were compared. These DVHs were extracted from TPS and MC simulation dose distributions and comparisons were done with MATLAB and 3DSlicer.

Results

Linear accelerator modeling and model verification

Figure 1 illustrates the components' schematic diagram of the LINAC head for both energies. The PDDs and the dose profiles were drawn at 10-cm depth for three different field sizes in two-photon energies with and without wedge which were calculated and measured with MC and experimental measurement, respectively. We have only presented the PDD and the dose profiles of the MC simulation results for reference field size in two-photon energies, with and without wedge [Figure 2].

The initial electron source for both nominal energies had a Gaussian distribution with a mean energy of 6.25 MeV and 14.9 MeV, respectively. The full width at half maximum (FWHM) for 6 MV was 3.3% (0.2083 MeV) with a spatial distribution on the central axis modeled by a Gaussian function with 0.8° FWHM. Nevertheless, for 15 MV, Gaussian energy distributions had a half width at half maximum of 4 MeV in the minimum direction and its spatial distribution at the central axis was 0.2 cm. The nominal energy with the above parameters in MC has a good agreement with experimental measurements according to the gamma index calculation with 2%/2 mm criteria for all field sizes. The uncertainty for all voxels used to estimate PDDs and dose profiles was <2%.

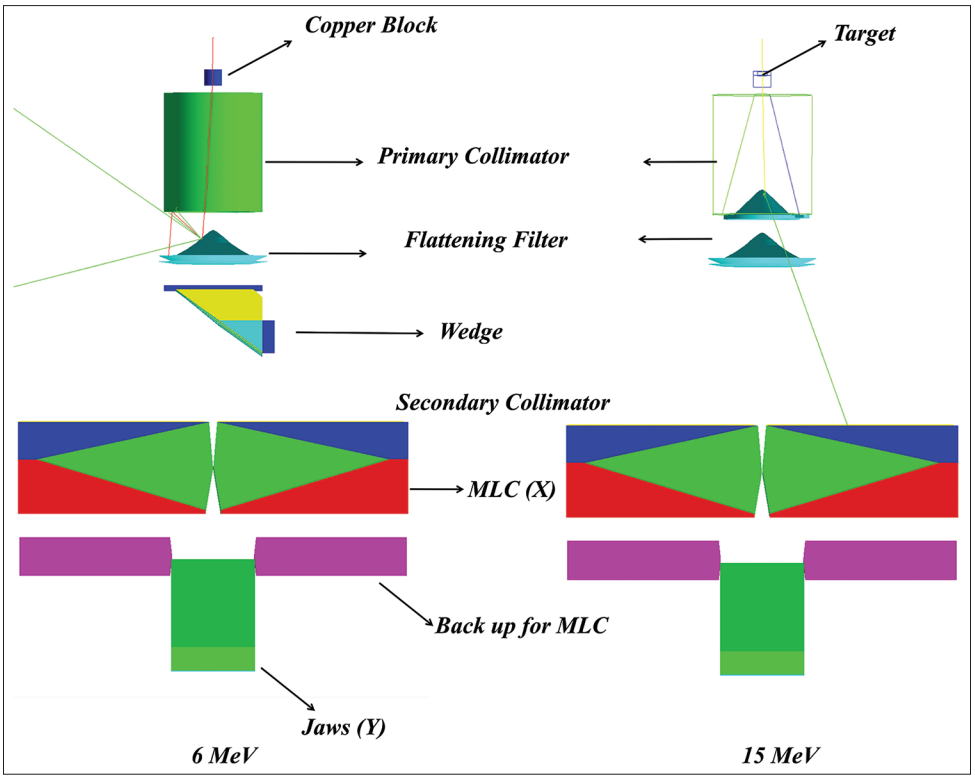

Figure 1: A schematic geometry of Elekta Precise LINAC head: (a) 6 MV, (b) 15 MV

RANDO phantom in Monte Carlo simulation of treatment plans

In regard to comparing the normalized dose distribution for the TPS and MC simulation with gamma index tools, more than 90% of voxels will pass the gamma index test with 6%/4 mm criteria for all plans. The gamma index results for different criteria are written in Table 2. These criteria are acceptable for the following reasons: (1) MC codes are more precise than TPS and different algorithms in TPS will affect the dose distribution, and (2) Treatment plans for breast cancer are one of the most complicated plans in radiotherapy that have inhomogeneity and different interfaces with air and bones in the thorax. Therefore, having more DD and DTA criteria in the gamma index would be acceptable. The gamma index results (with 4%/4 mm criteria) for one slice of different plans were plotted with MATLAB [Figures 3 and 4].

CTV DVHs for all eight plans in two energies and four techniques (6 and 15 MV) are depicted in Figures 5 and 6, respectively. Following Figures 5 and 6 and Table 3 which represented the properties of CTV DVH such as average, maximum, minimum dose, and $D_{95\%}$ for 6 and 15 MV photon mode energies are reported. Table 3 compares the parameters for MC and TPS CTVs DVH results in four treatment plans.

Out-of-field photon dose distribution verification

The results of point doses in MC simulation dose distribution extracted from the 3DSlicer and the DD between point dose measurement[31] and MC simulation results are tabulated in Tables 4 and 5, respectively.

The numbers in Table 4 show the mean and standard deviation based on 50 Gy in 25 fractions (2 Gy per fraction). After passing the criteria, the DVHs for all the organs that were initially contoured plus the right and left femur were calculated and compared with the TPS' DVHs. To reduce the number of figures in the article, the heart and left lung for all eight plans (6 and 15 MV) are depicted in Figures 7-10, respectively. As shown in these figures, the low dose part of DVHs was illustrated to demonstrate the results more accurately. This type of illustration of DVHs was extracted from Joosten *et al*.[16]

Discussion

LINAC modeling and verification of model

According to Figure 2, the simulation has a high agreement with experimental measurement results even in the build-up region. Although the value of the gamma index is >1 at several points in the dose profiles penumbra region, the number of these points is limited. Based on PDDs and dose profile results, the LINAC model was verified and the code is ready for the other steps.

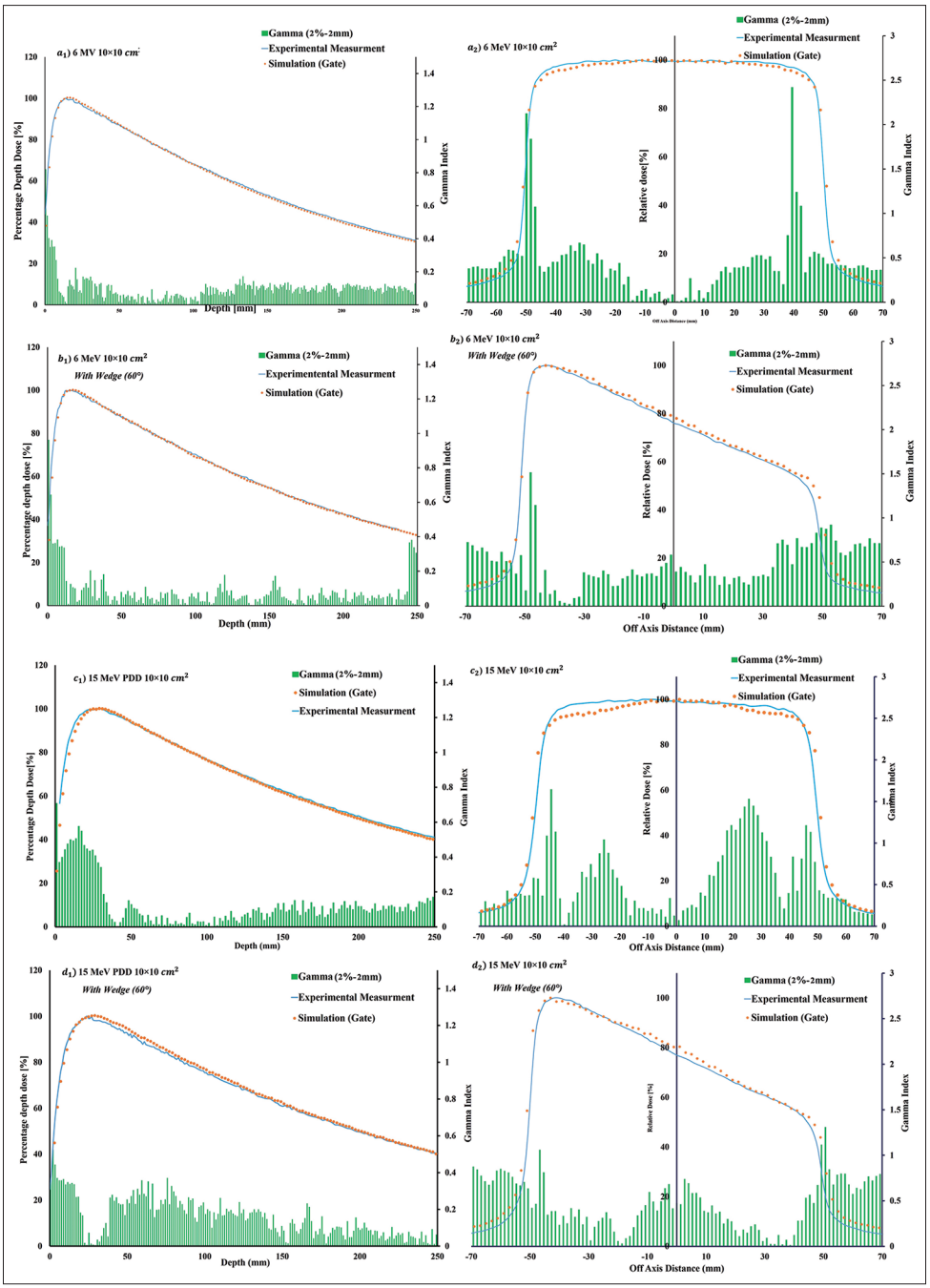

Figure 2: (2-1) Reference field size (10 cm × 10 cm), (a_1) percentage depth dose (PDD), 6 MV, without wedge, (a_2) Dose profile, 6MV, without wedge, (b_1) PDD, 6 MV, with wedge, (b_2) Dose profile, 6MV, without wedge. (2-2) Reference field size (10 cm × 10 cm), (c_1) PDD, 15 MV, without wedge, (c_2) Dose profile, 15 MV, without wedge, (d_1) PDD, 15 MV, with wedge, (d_2) Dose profile, 15 MV, with wedge. PDD: Percentage depth dose

RANDO phantom in Monte Carlo simulation of treatment plans

Since the TPSs are used different algorithms for dose calculation and the different studies' results show that the dose distribution calculation with MC simulation is more precise than the TPSs and even in some cases, TPSs have overestimated the dose distribution,[34-39] therefore, the gamma index criteria are evaluated for criteria which are bigger than 3%/3 mm. On the other hand, the 3%/3 mm criteria and smaller ones were recommended for comparing MC results and experimental measurement, not for treatment plan verification which is more complicated in dose calculation algorithms, patient setups such as the gantry, collimator, and table angles, and the presence of wedge and shield in treatment field. The presence of each one alone can cause more differences in dose distribution calculations. In addition to the explained reasons, the authors know that in patients with breast cancer, the target tissue for radiation therapy and the planning

Table 1: Eight different treatment plans were performed on RANDO phantom, Experimental measurement with thermoluminescent dosimeters, and Monte Carlo simulation

Plan	Energy																							
	6 MV												15 MV											
	Technique																							
	Conventional						Conformal						Conventional						Conformal					
	2 opposed tangential fields		2 opposed tangential fields plus super clave and postaxial				2 opposed tangential fields		2 opposed tangential fields plus super clave and postaxial				2 opposed tangential fields		2 opposed tangential fields plus super clave and postaxial				2 opposed tangential fields		2 opposed tangential fields plus super clave and postaxial			
Name of field																								
Field size																								
X_1	−100	−100	−179	0	0	−108	−90	−96	−179	0	0	−108	−100	−100	−58	−51	0	−108	−90	−96	−58	−51	0	−108
X_2	100	100	0	179	99	0	90	92	0	179	99	0	100	100	51	63	99	0	97	92	51	63	99	0
Y_1	−57.5	60	−50.5	−50.5	−30.5	−10.5	−50.5	−50.5	−50.5	−50.5	−30.5	−10.5	−57.5	60	−179	−179	−30.5	−10.5	−50.5	−50.5	−179	−179	−30.5	−10.5
Y_2	57.5	60	58	63	103.5	120.5	53	60.5	58	63	103	120.5	57.5	60	0	0	103.5	120.5	53	60.5	0	0	103.5	120.5
Gantry angle	298	118	298	118	350	170	298	118	298	118	350	170	298	118	298	118	350	170	298	118	298	118	350	170
Collimator angle	96	264	96	264	90	270	96	264	96	264	90	270	96	264	6	354	90	270	96	264	6	354	90	270
Couch rotation	0	0	0	0	0	0	0	0	0	0	0	0	0	0	0	0	0	0	0	0	0	0	0	0
Wedge	Yes	Yes	Yes	Yes	No	No	Yes	Yes	Yes	Yes	No	No	No	No	No	No	No	No	No	No	No	No	No	No
Block	No	No	No	No	Yes	Yes	No	No	No	No	No	No	No	No	No	No	No	No	No	No	No	No	No	No
MLC	No	No	No	No	No	No	Yes	Yes	Yes	Yes	Yes	Yes	No	No	No	No	No	No	Yes	Yes	Yes	Yes	Yes	Yes

The dimension of lengths and angles is millimeters and degree, respectively. MLC – Multi-leaf collimator

Table 2: Gamma index results for different plans with 6 and 15 MV energy

Energy	Technique	Gamma criteria				
		3%, 3 mm	6%, 3 mm	6%, 4 mm	6%, 5 mm	6%, 6 mm
15 MV	Conformal	76.43	82.91	90.13	94.93	98.64
	Conventional	80.60	86.47	92.93	96.88	99.12
	Conformal + supra	77.58	87.75	96.25	98.86	99.36
	Conventional + supra	84.50	90.49	96.46	99.25	99.97
6 MV	Conformal	82.49	87.12	93.11	96.17	98.21
	Conventional	85.11	90.63	95.16	97.58	99.16
	Conformal + supra	77.66	83.02	89.77	93.63	95.52
	Conventional + supra	79.79	86.07	93.10	95.97	97.08

Table 3: Clinical tumor volume's dose volume histogram properties for 6 MV and 15 MV photon mode energies, Monte Carlo and treatment planning system dose calculation methods and four treatment plans

Dose (Gy)	Technique	Energy							
		6 MV				15 MV			
		Average	Minimum	Maximum	$D_{95\%}$	Average	Minimum	Maximum	$D_{95\%}$
Conventional (2 tang)	TPS	50.31	0.00	56.82	43.3	52.98	0.00	56.89	44.50
	MC	50.61	18.34	55.58	45.10	52.77	19.78	58.13	42.90
Conventional (2 tang + axilla)	TPS	50.11	0.00	55.63	43.50	53.59	0.00	58.85	45.10
	MC	50.04	14.77	55.10	43.90	53.41	7.25	60.04	42.10
Conformal (2 tang)	TPS	50.65	0.00	56.58	44.80	53.97	0.00	58.20	45.00
	MC	50.77	3.35	56.32	44.30	53.68	5.19	59.54	42.50
Conformal (2 tang + axilla)	TPS	49.76	0.00	53.91	44.00	53.97	0.00	58.86	45.10
	MC	49.90	16.65	55.50	44.30	54.16	7.02	59.50	43.20

TPS – Treatment planning system; MC – Monte Carlo

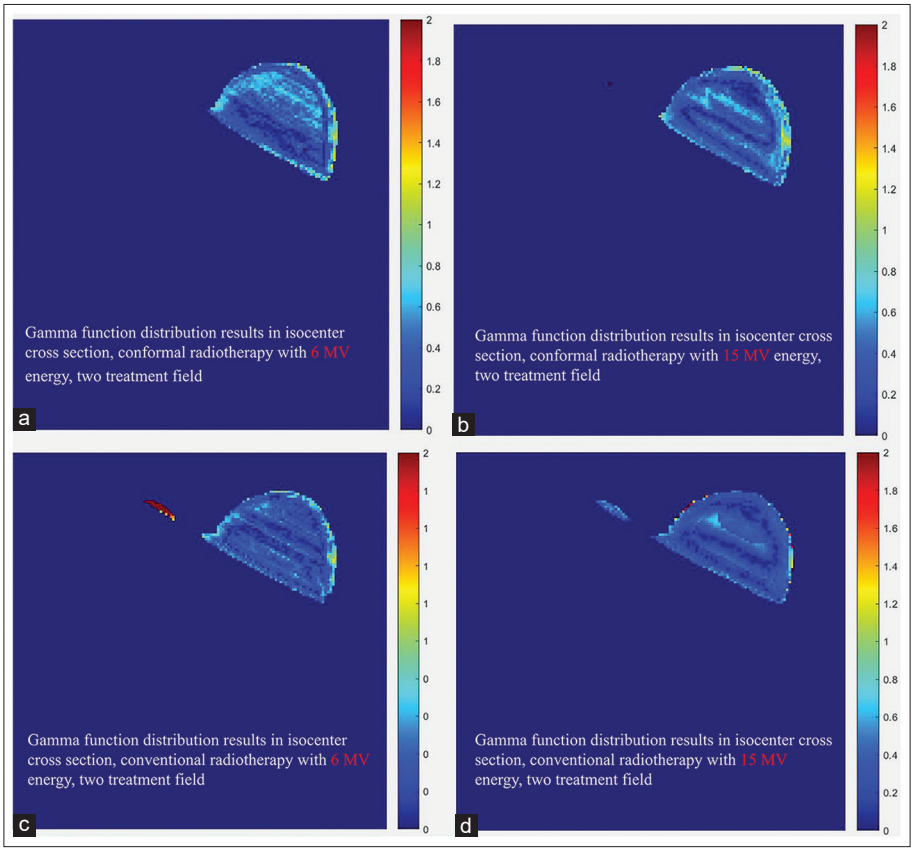

Figure 3: Gamma function distribution results in the cross-section of isocenter in the treatment planes with two treatment fields: (a) Conformal technique with 6 MV, (b) Conformal technique with 15 MV, (c) Conventional technique with 6 MV, (d) Conventional technique with 15 MV

Table 4: The point dose's results in Monte Carlo dose distribution which was extracted with three-dimensional slicer

Techniques organs	Energy							
	6 MV				15 MV			
	Conventional (2 tang)	Conformal (2 tang)	Conventional (2 tang + axilla)	Conformal (2 tang + axilla)	Conventional (2 tang)	Conformal (2 tang)	Conventional (2 tang + axilla)	Conformal (2 tang + axilla)
Left lens	241.00±23.50	171.00±47.00	702.50±4.00	651.50±23.75	203.00±12.50	251.50±8.25	640.75±16.25	492.50±15.75
Right lens	220.00±20.00	104.25±11.25	553.75±4.00	480.75±25.75	239.75±8.00	228.25±11.25	527.00±49.75	409.25±8.50
Thyroid	420.75±12.25	264.75±30.50	2966.00±19.75	277500±22.50	435.50±7.75	376.50±7.25	2942.25±149.00	2951.75±15.75
	587.50±23.50	327.00±71.50	53388.00±294.25	63252.25±959.00	441.00±16.00	420.00±7.25	44553.75±186.00	49416.00±690.25
Left lung	317.05±4.00	165.25±13.00	63023.75±732.75	66311.25±274.00	237.00±9.00	227.25±3.75	56715.50±889.25	58791.25±3740.25
	687.50±22.25	303.25±14.50	51597.25±1482.50	30834.50±2153.50	403.25±2.00	437.50±14.25	9952.75±285.25	27692.00±421.25
	438.50±18.00	229.00±13.75	4715.25±1335.3	4658.75±121.75	352.25±4.75	337.00±10.50	3812.75±84.75	5257.00±191.50
	1900.50±49.00	1611.75±52.25	1611.75±68.75	2190.75±13.25	1029.50±13.25	931.25±8.50	1619.75±17.25	1727.00±2.50
	1608.00±88.50	1112.00±101.00	1950.25±12.75	1763.50±26.00	1189.00±8.50	1201.75±8.50	1807.00±7.25	2014.00±34.50
Right lung	245.75±12.00	137.50±10.25	1313.00±23.00	1155.50±32.75	214.50±7.50	271.00±3.00	896.00±35.25	904.75±13.75
	323.75±7.25	177.75±6.25	958.75±25.25	963.00±24.25	243.25±4.25	224.25±2.50	720.50±7.75	784.25±10.75
	462.00±13.25	293.50±5.50	579.75±7.50	730.50±5.50	331.00±0.50	356.75±9.25	522.50±12.25	521.75±12.25
	479.25±7.00	459.50±21.50	734.75±18.75	665.75±8.75	336.00±10.50	362.00±4.25	645.75±1.00	678.50±10.50
	344.00±17.45	274.50±13.00	549.50±4.50	461.50±2.50	217.75±7.25	260.00±9.50	557.25±17.75	492.25±26.75
Spinal cord	237.75±7.5	148.25±6.00	2195.25±8.75	1884.0±3.00	190.25±2.75	275.25±3.75	1472.25±80.00	1463.75±15.25
	271.25±16.00	134.50±6.25	24188.75±1089.50	19243.00±242.25	176.75±2.50	204.75±5.50	18124.25±853.25	21303.50±284.00
	298.00±8.50	180.50±15.05	3635.75±347.00	4663.25±228.50	278.50±2.00	253.50±7.00	2368.75±17.50	4606.00±41.75
	219.25±5.75	129.25±7.00	1334.75±26.50	1263.25±35.75	162.50±2.75	175.00±3.75	916.75±24.25	1042.50±33.25
	261.5±9.00	22.75±11.25	665.00±19.50	661.50±21.25	175.25±3.25	228.50±7.75	598.00±33.25	557.75±11.00
	348.50±8.75	213.75±10.50	1062.00±9.50	839.50±12.75	239.00±10.00	252.75±3.50	901.00±14.25	880.00±11.75
Heart	1146.00±53.25	860.75±18.75	1630.25±47.25	1569.00±31.00	746.50±17.50	731.25±25.50	1268.00±15.25	1430.75±37.25
	1583.00±79.75	1346.00±41.75	2375.00±5.00	2194.25±16.00	1061.25±13.70	1071.75±11.50	1621.00±25.50	1899.00±46.00
	739.75±17.75	528.50±23.75	1248.75±25.00	1141.75±11.75	503.75±10.50	454.00±12.25	992.75±9.75	1054.50±20.00
	1250.25±41.75	1154.75±15.75	1716.25±30.25	1512.75±17.50	793.75±14.50	808.25±6.00	1306.75±51.50	1386.00±12.75
	949.25±29.00	828.00±22.75	1601.75±32.25	1423.75±7.50	649.75±11.75	645.00±7.75	1265.75±24.25	1348.25±34.25
	722.50±11.75	611.25±24.75	1231.50±114.00	1084.50±45.00	490.75±17.25	504.50±3.75	944.25±19.75	973.75±34.50
Liver	395.00±9.25	450.25±18.25	585.25±11.25	522.25±7.50	337.75±4.50	364.50±7.25	591.75±1.75	554.00±19.00
	487.00±24.00	264.25±66.25	658.75±13.75	577.00±14.00	334.50±2.25	342.25±7.25	653.00±7.75	643.50±5.25
	824.50±30.75	924.50±32.25	929.50±3.25	807.75±14.00	491.50±5.50	588.50±2.00	787.75±24.25	848.25±32.00
	923.00±32.00	1266.50±28.50	1203.00±25.50	1029.00±18.00	623.75±1.25	663.50±15.25	1028.25±13.75	1348.25±34.25
	311.25±8.25	369.25±15.25	439.755±4.25	380.00±3.00	217.25±4.25	244.25±7.00	421.00±9.75	973.75±34.50
Right kidney	195.50±13.25	172.50±6.50	259.25±11.75	292.00±11.50	127.75±2.50	156.75±4.50	268.00±10.25	250.75±10.25
	243.75±3.00	289.25±17.50	388.50±14.25	314.50±8.50	203.00±1.25	207.75±6.75	351.75±2.75	327.25±6.75
	224.75±1.25	243.00±11.00	339.75±14.25	261.25±2.50	191.50±4.00	181.75±8.75	291.25±7.25	318.50±18.50

Contd...

Table 4: Contd...

Techniques organs	Energy							
	6 MV				15 MV			
	Conventional (2 tang)	Conformal (2 tang)	Conventional (2 tang + axilla)	Conformal (2 tang + axilla)	Conventional (2 tang)	Conformal (2 tang)	Conventional (2 tang + axilla)	Conformal (2 tang + axilla)
Left kidney	274.00±2.50	355.00±7.50	464.00±18.25	383.00±8.00	234.75±4.00	210.25±2.50	407.50±5.75	402.25±6.75
	403.75±14.75	450.25±8.75	529.25±15.25	473.50±15.25	237.25±1.75	256.75±6.75	451.75±3.00	430.25±21.00
	293.25±9.25	390.00±5.50	418.75±3.50	355.75±7.75	227.75±1.75	219.50±3.50	389.75±0.50	323.75±10.00
Rectum	89.25±8.00	94.75±6.75	123.00±14.25	122.25±9.00	85.50±2.25	78.00±2.00	112.25±5.50	110.25±7.75
	122.50±8.75	89.00±11.25	115.50±6.00	131.00±11.00	89.25±6.75	81.75±6.75	109.25±6.75	114.50±8.00
Bladder	82.75±9.50	81.50±2.25	115.00±5.25	117.75±5.75	73.00±0.50	75.25±0.50	100.75±7.00	118.00±9.50
	67.25±4.75	82.50±1.75	108.25±3.00	111.25±5.50	76.25±2.25	77.00±0.75	107.00±7.75	110.75±5.25
	56.75±2.00	75.00±5.50	103.75±4.25	115.50±5.25	73.50±5.00	76.00±1.50	100.25±5.00	111.25±7.75
	92.50±5.50	75.00±5.50	99.25±2.50	116.75±8.75	70.00±3.00	73.00±0.50	107.50±5.50	115.25±8.00
Uterine	78.80±5.50	79.50±3.00	101.50±3.75	120.00±5.00	73.75±1.50	76.50±2.50	103.00±7.75	9.16±8.00
	83.25±3.00	33.75±2.25	106.75±10.50	116.75±6.60	77.00±2.25	74.50±1.00	103.75±6.25	106.50±7.00
	67.50±11.25	71.75±3.00	97.25±5.00	111.75±7.25	71.00±4.75	67.75±1.00	105.50±5.25	113.75±8.00

target volume (PTV), unlike the other tumors such as the prostate and rectum that are located in the center of the body, is located at the edge of the body surface. Therefore, the treatment planning is more difficult and the uncertainties in dose calculation on the side of the PTV decreased.

Figures 3 and 4 demonstrate that the maximum differences are related to the edge of the body surface, the treatment field, or the edge of the shield. At the end of this stage, the CTV DVHs for all plans were calculated with 3DSlicer and compared with TPS DVHs. As indicated in Figures 5 and 6, the CTV DVHs for all eight plans in two energies and four techniques (6 and 15 MV) have a high agreement.

Out-of-field photon dose distribution verification

In the last step, the MC simulation for out-of-field point doses and OARs DVHs were compared with the previous study[31] TLDs results and TPS's DVHs, respectively. The MC simulation results in Table 4 verified the experimental measurement results in the previous study.[31] Table 4 indicates that the point doses in close organs are more than in the far organs. This table proves that 15 MV photon compared to the 6 MV photon energy penetrates more and has less scatter radiation. Due to the wide treatment plans in conventional plans (conformal in the presence of a dedicated shield) compared to the conformal plans, point doses in these plans are more than in the conformal plans. However, MLC in conformal plans or wedge in conventional plans caused more scatter radiation which affected in results. Table 4 expresses the same result discussed in the previous study about the experimental measurement.[31] They will not be repeated to shorten the article.

As demonstrated in Table 5, 83.33% of out-of-field point doses have a difference of <5%, 4.9% of out-field point doses have a difference bigger than 7%, and the maximum difference between MC out-of-field point dose and TLD results was 9.79%. This difference could be due to the comparison of the average point dose measured with the average point dose of several voxels at the dosimeter position in the phantom. For extracting the point dose in phantom, an average of the dose for several points is taken in the position of the TLD, so this causes the difference to be less and even more in some points. On the other hand, all measuring methods and tools have their own systematic and statistical errors, and TLDs are no exception to this rule.

The results of the experimental and simulation dosimetry point doses are comparable to the results which were presented in Berris *et al.* study.[27] In the Berris research Table 2, the average dose received to the out-of-field organs for two different field sizes of breast cancer with two tangent fields was reported, and these average doses are comparable with the average dose received to the

Table 5: The dose difference between point dose measurement in the previous article[31] and Monte Carlo results

Techniques organs	Energy							
	6 MV				15 MV			
	Conventional (2 tang)	Conformal (2 tang)	Conventional (2 tang + axilla)	Conformal (2 tang + axilla)	Conventional (2 tang)	Conformal (2 tang)	Conventional (2 tang + axilla)	Conformal (2 tang + axilla)
Left lens	4.18	0.39	0.23	5.77	5.90	6.03	1.53	0.15
Right lens	0.76	5.27	0.19	1.26	0.14	0.73	5.25	1.73
Thyroid	7.21	2.43	0.86	0.22	0.50	4.51	2.87	0.12
	1.03	9.08	1.62	0.91	0.19	2.29	7.03	5.27
Left lung	3.36	6.52	0.56	0.48	1.30	3.49	3.78	8.70
	0.00	6.08	0.03	0.40	0.02	2.58	0.56	0.32
	0.00	5.40	0.11	1.05	5.16	3.24	1.06	0.11
	3.90	0.22	0.86	1.09	0.45	0.11	0.76	0.18
	3.13	1.00	0.48	0.35	0.25	1.81	0.68	1.08
Right lung	4.24	7.64	0.14	2.13	5.25	1.73	0.30	1.31
	3.99	7.08	0.09	0.72	0.28	2.79	1.32	0.30
	4.54	9.30	2.48	0.86	0.0	1.22	0.31	1.72
	3.74	1.95	1.36	0.82	1.97	0.07	0.38	1.34
	8.96	0.93	0.16	1.46	0.63	1.93	0.13	2.10
Spinal cord	0.32	0.99	7.93	0.18	2.85	2.58	2.27	0.24
	3.92	3.38	0.14	0.58	0.84	1.77	3.96	0.86
	5.79	4.89	0.07	2.72	2.56	5.77	1.57	9.29
	5.13	3.97	3.99	0.83	3.57	6.23	1.25	0.35
	3.81	0.13	0.57	1.56	7.13	5.88	1.96	0.07
	1.03	3.98	0.23	0.59	4.96	3.86	1.26	2.46
Heart	1.23	1.36	0.27	0.54	1.19	0.04	2.31	1.57
	1.24	0.29	0.17	0.71	0.46	0.48	1.74	0.03
	0.87	1.48	0.34	0.20	3.34	0.87	0.13	0.01
	0.05	0.62	0.03	0.15	1.81	0.71	1.64	0.35
	1.06	0.19	0.33	0.31	0.02	0.44	0.15	0.07
	1.13	1.00	7.31	5.71	0.48	0.41	0.88	2.46
Liver	3.87	0.01	1.20	1.79	1.41	0.64	0.09	0.95
	3.01	2.07	2.16	1.59	0.02	0.99	0.33	0.41
	2.16	1.49	0.54	0.46	1.44	0.57	0.62	1.80
	0.61	1.76	0.46	1.84	1.02	0.85	1.09	0.62
	1.26	1.77	0.86	0.08	4.43	1.58	3.02	2.33
Right kidney	0.86	1.64	2.25	8.11	5.08	0.01	3.86	2.40
	0.17	1.34	1.73	0.47	0.27	2.41	1.29	0.92
	2.81	1.85	1.99	3.48	0.89	0.16	0.18	5.08
Left kidney	5.70	4.07	0.33	1.19	2.33	5.86	3.43	2.57
	3.50	2.57	1.03	0.08	3.66	0.04	3.63	3.55
	0.25	1.12	0.72	1.51	0.89	8.68	3.45	1.47
Rectum	2.61	2.85	7.49	0.75	1.20	8.98	5.32	6.80
	1.72	0.60	2.72	5.80	9.79	1.30	6.15	4.57
Bladder	0.40	3.63	4.84	2.58	5.24	0.20	4.27	2.95
	4.89	9.15	5.89	6.72	6.67	3.16	4.05	4.26
	6.59	1.64	2.03	3.70	2.74	0.84	4.05	0.82
	1.05	3.63	1.61	5.63	4.00	0.30	3.56	4.69
Uterine	2.10	1.89	1.68	8.45	1.37	4.17	0.21	2.86
	0.4	0.74	0.13	1.92	1.84	2.23	5.47	5.97
	4.40	0.18	5.14	4.19	1.12	2.31	4.65	3.62

out-of-field organs of this study. As the results demonstrate, the agreement between the results of the present study and the Berris *et al*. study is above 90%.

Based on the DVHs' out-field organs, especially for the organs which received high doses, there is a great agreement between the TPS and MC simulation for doses above 20 Gy.

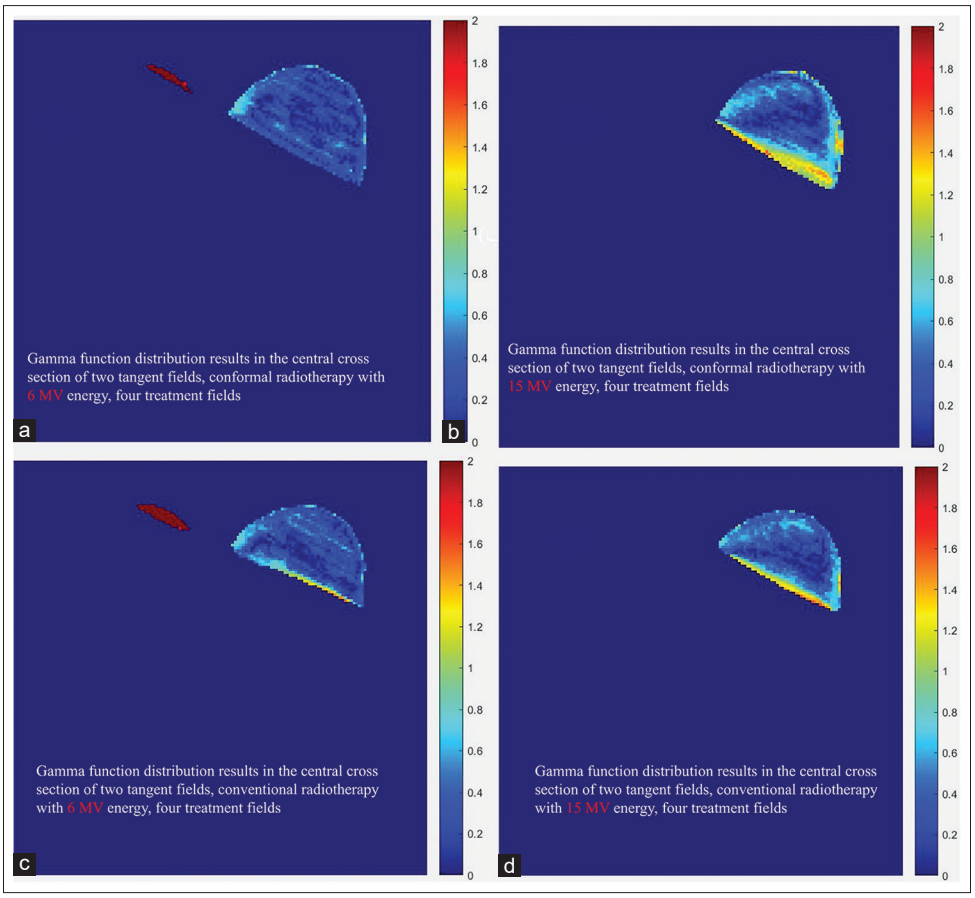

Figure 4: Gamma function distribution results in the cross-section of isocenter in the treatment planes with four treatment fields: (a) Conformal technique with 6 MV, (b) Conformal technique with 15 MV, (c) Conventional technique with 6 MV, (d) Conventional technique with 15 MV

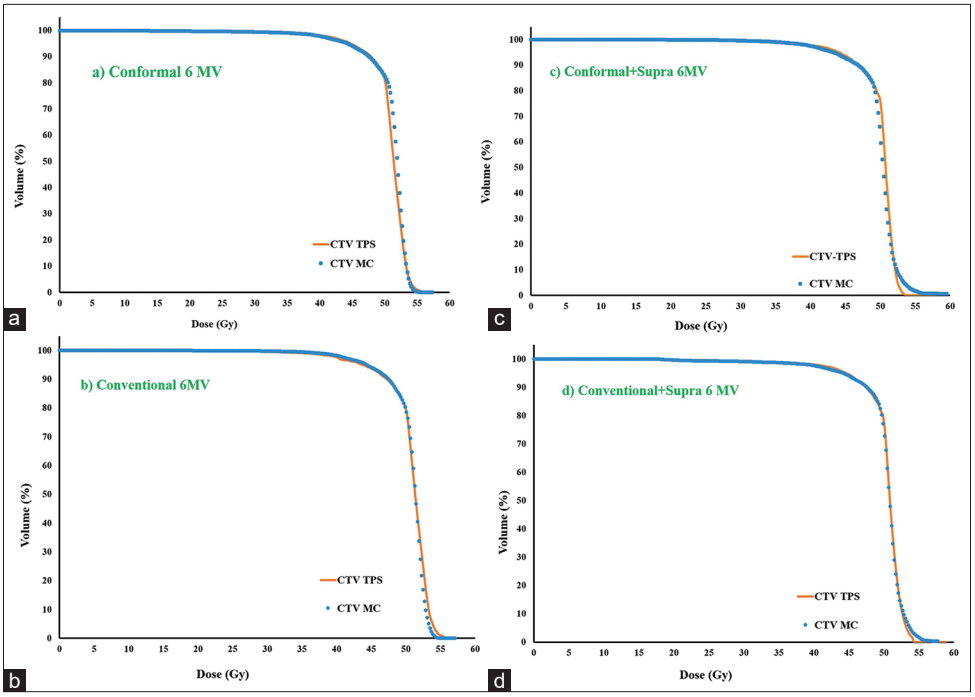

Figure 5: Clinical tumor volume's dose volume histograms comparison with Monte Carlo and treatment planning system for 6MV plans (a) Conformal technique, (b) Conventional technique, (c) Conformal + supra technique, (d) Conventional + supra technique

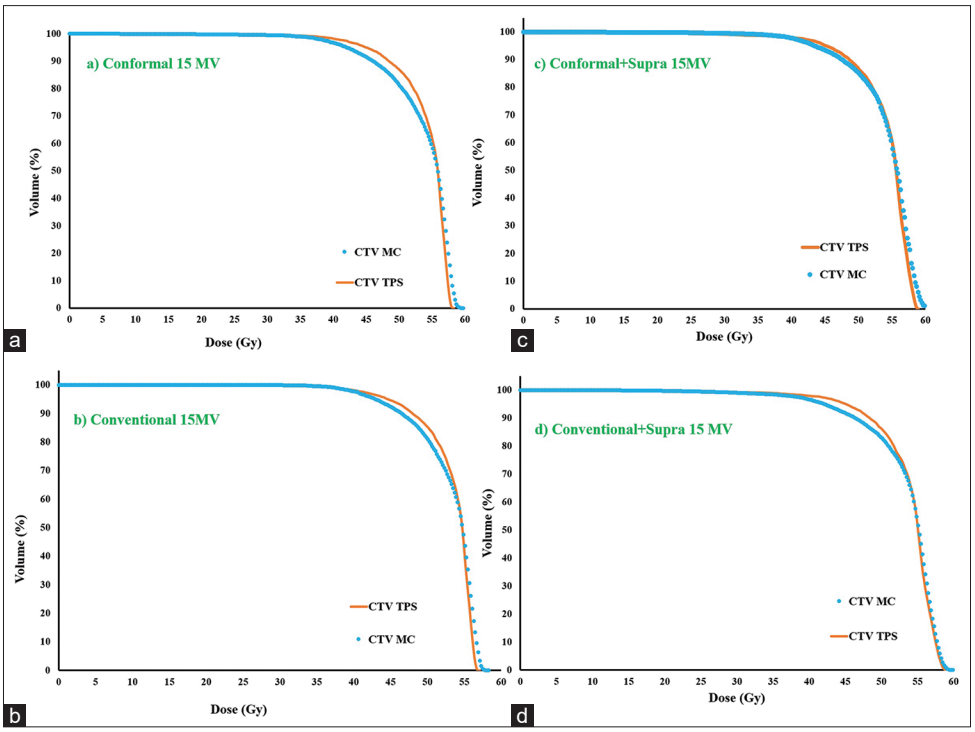

Figure 6: Clinical tumor volume's dose volume histograms comparison with Monte Carlo and treatment planning system for 15 MV plans (a) Conformal technique, (b) Conventional technique, (c) Conformal + supra technique, (d) Conventional + supra technique

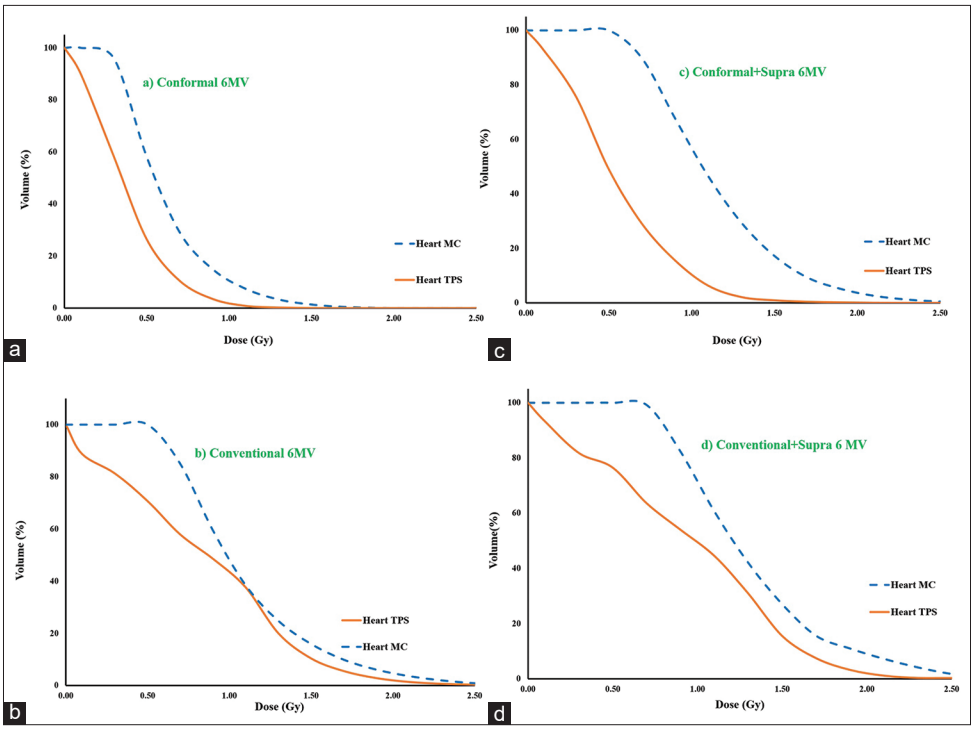

Figure 7: Heart's dose volume histograms comparison with Monte Carlo and treatment planning system for 6MV plans (a) Conformal technique, (b) Conventional technique, (c) Conformal + supra technique, (d) Conventional + supra technique

On the other hand, there is a slight difference and large difference for doses between 5 and 20 Gy and <5 Gy (low dose part), respectively. This difference reaches 70% for the low-dose part. These differences in DVHs are due to the inability of TPS to calculate out-of-field organ dose distribution. The DVH's characteristics for MC and TPS results are presented for a better comparison in Table 3. The results of different studies[13,16,26,27] about the inability

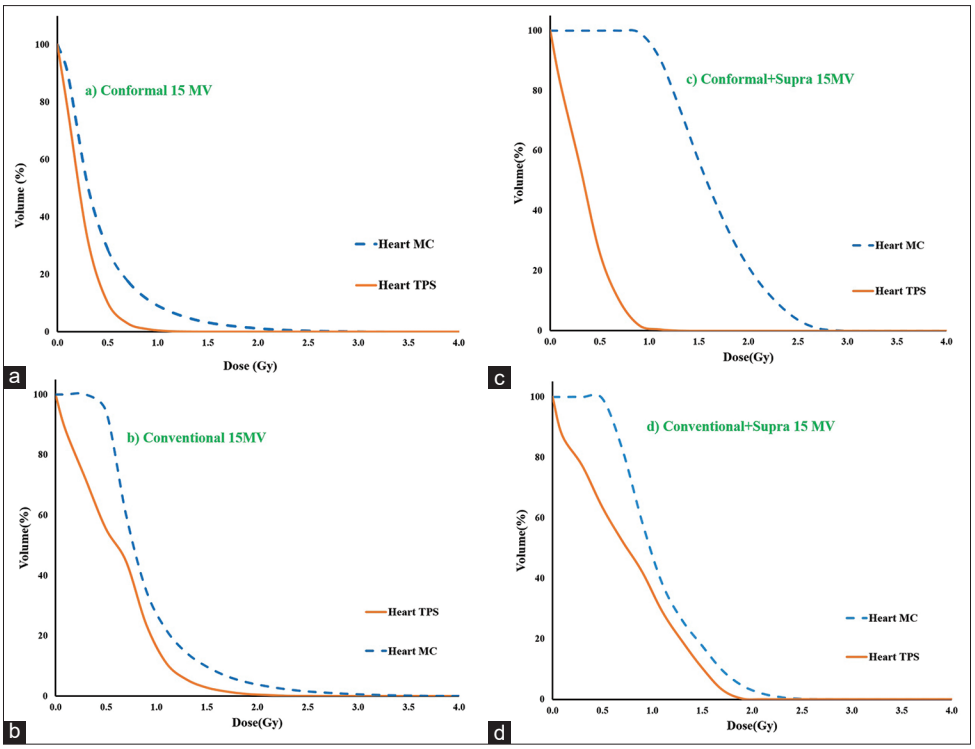

Figure 8: Heart's dose volume histograms comparison with Monte Carlo and treatment planning system for 15 MV plans (a) Conformal technique, (b) Conventional technique, (c) Conformal + supra technique, (d) Conventional + supra technique

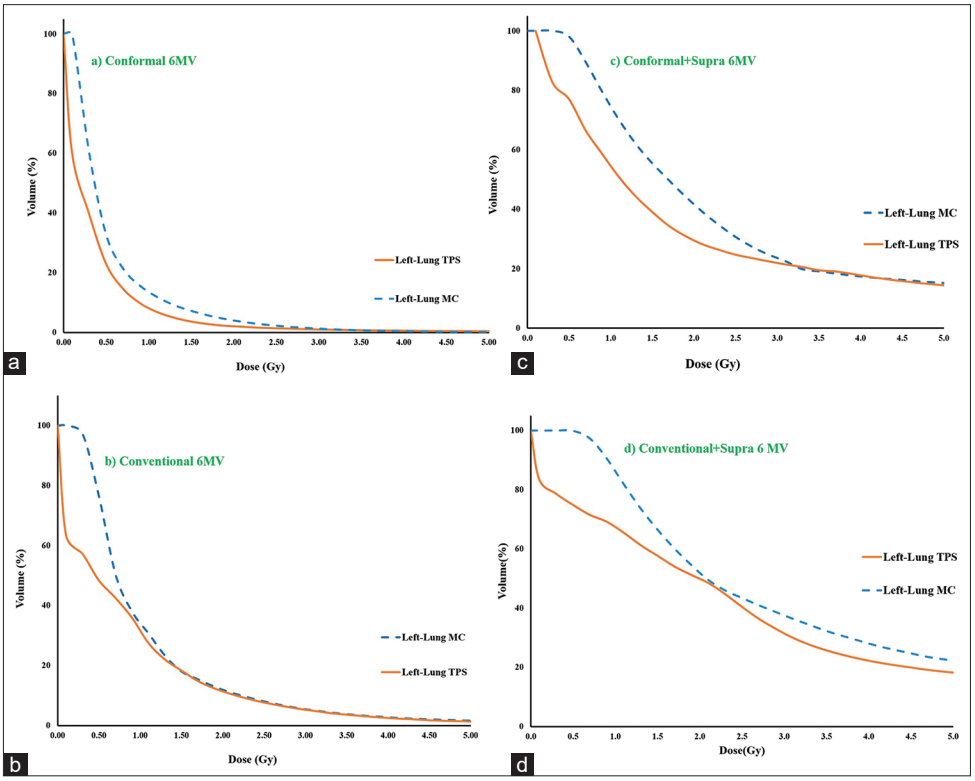

Figure 9: Left lung's dose volume histograms comparison with Monte Carlo and treatment planning system for 6MV plans (a) Conformal technique, (b) Conventional technique, (c) Conformal + supra technique, (d) Conventional + supra technique

of the TPS for calculating the out-field dose confirm the accuracy of this research results.

Another reason for observing this difference in dose distribution between the TPS and MC simulation

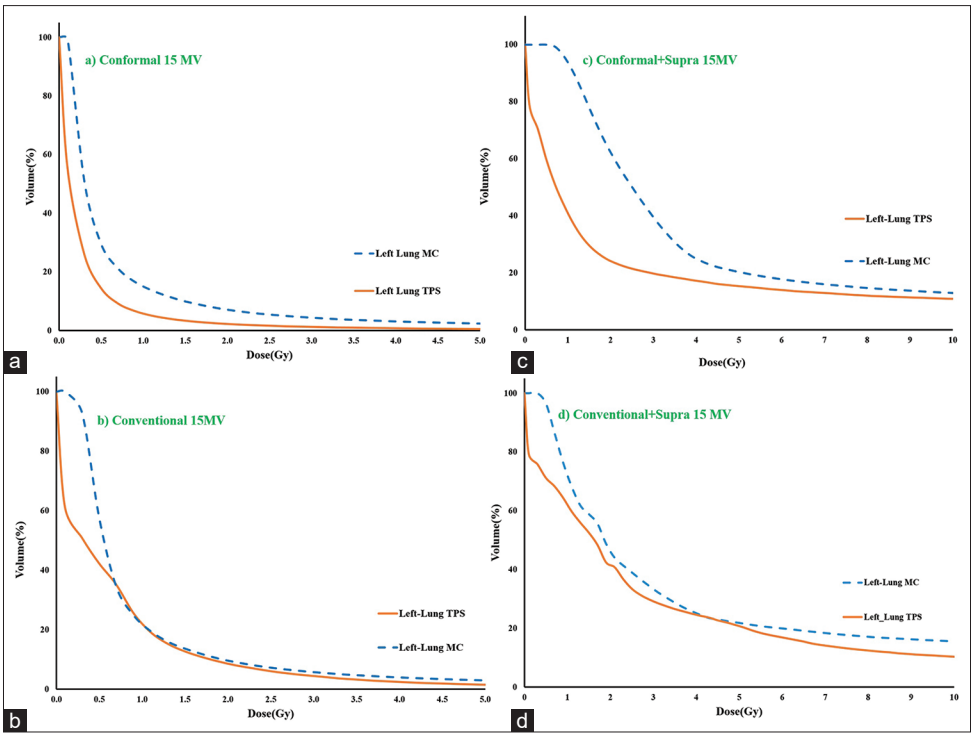

Figure 10: Left lung's dose volume histograms comparison with Monte Carlo and treatment planning system for 6MV plans (a) Conformal technique, (b) Conventional technique, (c) Conformal + supra technique, (d) Conventional + supra technique

calculation can be attributed to the scattered rays from the LINAC head. In the TPS algorithm, the radiation scattering caused by the patient is considered, while the scattering caused by the LINAC head is not considered.[16] On the other hand, in the MC simulation for the dose distribution calculations electron contamination, the collimator leakage, and the scattering due to the presence of wedges in the field are considered, while they are usually not considered in the TPS dose calculation algorithm, or it has a constant value.[16]

Conclusion

The present study is an introduction to the risk calculation of complications due to radiotherapy, especially in secondary cancer research. One of the important factors for risk estimation is 3D-dose distribution determination in nontarget organs. Given that the TPS does not have the required ability to calculate the accurate dose distribution in out-of-field organs, the authors used MC simulation as an accurate tool for calculating complex situations in out-of-field organs in standard conditions.

Based on the authors' knowledge, different studies have been done to estimate the postradiation therapy risk and even mathematical models have been written for this calculation. However, in these studies, the average dose distribution or equivalent organ dose was used to calculate this risk and this causes a lower estimation. This underestimation will be more in organs that are close to the radiation field and a part of those organs receive a high dose. In the present study, an attempt has been made to calculate the 3D-dose distribution in the OAR, and by using this 3D-dose distribution, it is possible to check the possibility of postradiation therapy risk in the next studies.

Acknowledgments

The authors would like to thank Mashhad University of Medical Sciences for the financial support of this research. We are also thankful to the Radiation Therapy Department of Emam Reza Hospital for providing technical facilities.

Financial support and sponsorship

Nil.

Conflicts of interest

There are no conflicts of interest.

References

1. National Research Council. Health risks from exposure to low levels of ionizing radiation: BEIR VII phase 2. The National Academies Press, Washington, DC; 2006.
2. Howell R. Second primary cancers and cardiovascular disease after radiation therapy. NCRP report no. 170. Med Phys 2012;39:7729-31.
3. Schneider U. Mechanistic model of radiation-induced cancer after fractionated radiotherapy using the linear-quadratic formula. Med Phys 2009;36:1138-43.
4. Schneider U. Modeling the risk of secondary malignancies after radiotherapy. Genes (Basel) 2011;2:1033-49.
5. Schneider U, Sumila M, Robotka J, Gruber G, Mack A,

Besserer J. Dose-response relationship for breast cancer induction at radiotherapy dose. Radiat Oncol 2011;6:67.

6. Shuryak I, Hahnfeldt P, Hlatky L, Sachs RK, Brenner DJ. A new view of radiation-induced cancer: Integrating short-and long-term processes. Part I: Approach. Radiat Environ Biophys 2009;48:263-74.
7. Shuryak I, Hahnfeldt P, Hlatky L, Sachs RK, Brenner DJ. A new view of radiation-induced cancer: Integrating short-and long-term processes. Part II: Second cancer risk estimation. Radiat Environ Biophys 2009;48:275-86.
8. Sánchez-Nieto B, Medina-Ascanio KN, Rodríguez-Mongua JL, Doerner E, Espinoza I. Study of out-of-field dose in photon radiotherapy: A commercial treatment planning system versus measurements and Monte Carlo simulations. Med Phys 2020;47:4616-25.
9. Mazonakis M, Damilakis J. Out-of-field organ doses and associated risk of cancer development following radiation therapy with photons. Phys Med 2021;90:73-82.
10. Goy E, Tomezak M, Facchin C, Martin N, Bouchaert E, Benoit J, *et al.* The out-of-field dose in radiation therapy induces delayed tumorigenesis by senescence evasion. Elife 2022;11:e67190.
11. Benzazon N, Colnot J, de Kermenguy F, Achkar S, de Vathaire F, Deutsch E, *et al*. Analytical models for external photon beam radiotherapy out-of-field dose calculation: A scoping review. Front Oncol 2023;13:1197079.
12. Stovall M, Weathers R, Kasper C, Smith SA, Travis L, Ron E, *et al.* Dose reconstruction for therapeutic and diagnostic radiation exposures: Use in epidemiological studies. Radiat Res 2006;166:141-57.
13. Howell RM, Scarboro SB, Kry SF, Yaldo DZ. Accuracy of out-of-field dose calculations by a commercial treatment planning system. Phys Med Biol 2010;55:6999-7008.
14. Bahreyni Toossi MT, Soleymanifard S, Farhood B, Mohebbi S, Davenport D. Assessment of accuracy of out-of-field dose calculations by TiGRT treatment planning system in radiotherapy. J Cancer Res Ther 2018;14:634-9.
15. Huang JY, Followill DS, Wang XA, Kry SF. Accuracy and sources of error of out-of field dose calculations by a commercial treatment planning system for intensity-modulated radiation therapy treatments. J Appl Clin Med Phys 2013;14:4139.
16. Joosten A, Matzinger O, Jeanneret-Sozzi W, Bochud F, Moeckli R. Evaluation of organ-specific peripheral doses after 2-dimensional, 3-dimensional and hybrid intensity modulated radiation therapy for breast cancer based on Monte Carlo and convolution/superposition algorithms: Implications for secondary cancer risk assessment. Radiother Oncol 2013;106:33-41.
17. Wang L, Ding G×. Estimating the uncertainty of calculated out-of-field organ dose from a commercial treatment planning system. J Appl Clin Med Phys 2018;19:319-24.
18. Siji Cyriac T , Musthafa MM, Ganapathi Raman R, Abdul Haneefa K, Bhasi S. Out-of-field photon dosimetry study between 3-D conformal and intensity modulated radiation therapy in the management of prostate cancer. Int J Radiat Res 2015;13:127-34.
19. Sungkoo C, Seong Hoon K, Chan Hyeong K, Jang Guen PA, Jin Hyung PA, Jong Hwi J. Secondary cancer risks in out-of-field organs for 3-D conformal radiation therapy. Prog Nucl Sci Technol 2011;1:512-24.
20. Donovan EM, James H, Bonora M, Yarnold JR, Evans PM. Second cancer incidence risk estimates using BEIR VII models for standard and complex external beam radiotherapy for early breast cancer. Med Phys 2012;39:5814-24.
21. Oonsiri P, Vannavijit C, Wimolnoch M, Suriyapee S, Saksornchai K. Estimated radiation doses to ovarian and uterine organs in breast cancer irradiation using radio-photoluminescent glass dosimeters (RPLDs). J Med Radiat Sci 2021;68:167-74.
22. Howell RM, Scarboro SB, Taddei PJ, Krishnan S, Kry SF, Newhauser WD. Methodology for determining doses to in-field, out-of-field and partially in-field organs for late effects studies in photon radiotherapy. Phys Med Biol 2010;55:7009-23.
23. Vogel M, Gade J, Timm B, Schürmann M, Auerbach H, Nüsken F, *et al.* Comparison of breast cancer radiotherapy techniques regarding secondary cancer risk and normal tissue complication probability – Modelling and measurements using a 3D-printed phantom. Front Oncol 2022;12:892923.
24. Sánchez-Nieto B, Romero-Expósito M, Terrón JA, Irazola L, Paiusco M, Cagni E, *et al.* Intensity-modulated radiation therapy and volumetric modulated arc therapy versus conventional conformal techniques at high energy: Dose assessment and impact on second primary cancer in the out-of-field region. Rep Pract Oncol Radiother 2018;23:251-9.
25. Lee JA. Evaluation of the probability of secondary cancer during radiotherapy for prostate cancer. Educ Res (IJMCER) 2022;4:160-3.
26. Bednarz B, Hancox C, Xu XG. Calculated organ doses from selected prostate treatment plans using Monte Carlo simulations and an anatomically realistic computational phantom. Phys Med Biol 2009;54:5271-86.
27. Berris T, Mazonakis M, Stratakis J, Tzedakis A, Fasoulaki A, Damilakis J. Calculation of organ doses from breast cancer radiotherapy: A Monte Carlo study. J Appl Clin Med Phys 2013;14:4029.
28. Bednarz B, Xu XG. Monte Carlo modeling of a 6 and 18 MV varian clinac medical accelerator for in-field and out-of-field dose calculations: Development and validation. Phys Med Biol 2009;54:N43-57.
29. Luceski A, Laurent R, Gschwind R, De Conto C. Validation of the gate Monte Carlo code for radiation therapy and application to in homogeneities. Phys Med 2013;29:e23.
30. Wang L, Ding GX. The accuracy of the out-of-field dose calculations using a model based algorithm in a commercial treatment planning system. Phys Med Biol 2014;59:N113-28.
31. Behmadi M, Gholamhosseinian H, Mohammadi M, Naseri S, Momennezhad M, Bayani S, *et al.* Evaluation of breast cancer radiation therapy techniques in outfield organs of rando phantom with thermoluminescence dosimeter. J Biomed Phys Eng 2019;9:179-88.
32. Scherman JB. Developement and Evaluation of Methods for Comparison of Dose Distributions in Radiotherapy using Calculated, Synthetic and Simulated Measured Dose Distributions. Master's Thesis: Lunds Universiy; 2009.
33. Fedorov A, Beichel R, Kalpathy-Cramer J, Finet J, Fillion-Robin JC, Pujol S, *et al.* 3D slicer as an image computing platform for the quantitative imaging network. Magn Reson Imaging 2012;30:1323-41.
34. Kim SJ, Kim SK, Kim DH. Comparison of pencil-beam, collapsed-cone and Monte-Carlo algorithms in radiotherapy treatment planning for 6-MV photons. J Korean Phys Soc 2015;67:153-8.
35. Li JS, Pawlicki T, Deng J, Jiang SB, Mok E, Ma CM. Validation of a Monte Carlo dose calculation tool for radiotherapy treatment planning. Phys Med Biol 2000;45:2969-85.
36. Ojala JJ, Kapanen M. Quantification of dose differences between two versions of acuros XB algorithm compared to Monte Carlo simulations – The effect on clinical patient treatment planning. J Appl Clin Med Phys 2015;16:213-25.

37. Reynaert N, Van der Marck S, Schaart D, Van der Zee W, Van Vliet-Vroegindeweij C, Tomsej M, *et al.* Monte Carlo treatment planning for photon and electron beams. Radiat Phys Chem 2007;76:643-86.
38. Fipple MSchlegel W, Bortfeld T, Grosu AL. Monte Carlo Dose Calculation for Treatment Planning. New Technologies in Radiation Oncology Medical Radiology. Heidelberg Springer. 2006;197-206.
39. Wu VW, Tse TK, Ho CL, Yeung EC. A comparison between anisotropic analytical and multigrid superposition dose calculation algorithms in radiotherapy treatment planning. Med Dosim 2013;38:209-14.